euspen's 26th International Conference & Exhibition, Krakow, PL, June 2026
www.euspen.eu

# Evaluation of the temperature influence in the measurement uncertainty of a telescopic simultaneous ball-bar for manufacturing systems verification

Francisco Javier Brosed [1,2,3], Juan José Aguilar [1,2], Sergio Aguado [1,2], Marcos Pueo [1,2], Ana Cristina Majarena [1,2], Jesús Velázquez [1,2]

[1] *Department of Design and Manufacturing Engineering, University of Zaragoza, María de Luna 3, 50018 Zaragoza, Spain.*
[2] *Instituto de Investigación en Ingeniería de Aragón (I3A), 50018 Zaragoza, Spain*

[3] *fjbrosed@unizar.es*

**Abstract**
Machine tool and industrial robot verification processes increasingly demand higher accuracy due to the growing presence of high value-added operations in manufacturing. Several commercial solutions are currently available for the verification of manufacturing systems. Among them, telescopic systems are used to track the position of a manufacturing system by measuring three-dimensional coordinates. This verification can be performed using a single telescopic arm and tracking from three different positions, i.e. repeating the process three times, or by using three telescopic arms simultaneously to obtain the three-dimensional coordinates without repeating measurements. The work presented at euspen's ICE 2026 investigates the influence of temperature on the measurement results of an interferometry-based instrument using simultaneous multilateration. The measurement system consists of a telescopic simultaneous ball-bar composed of three telescopic arms that simultaneously measure the distances between three fixed reference spheres and a single moving sphere mounted on the spindle of a machine tool or on the end-effector of an industrial robot, which constitutes the manufacturing system under inspection. This study models the complete measurement process and the influence of temperature from the initial calibration steps—required to adjust each telescopic ball-bar—through to the final determination of the three-dimensional position. Intermediate measurement stages, such as the measurement of distances between the three fixed reference spheres using the telescopic ball-bars, are also included in the model.

Keywords: Interferometry; Measuring instrument;Thermal error;Verification

## 1. Introduction

Temperature significantly influences dimensional metrology through thermal expansion, causing parts and measurement tools to change size, creating errors relative to the 20°C standard, requiring compensation or controlled environments to maintain accuracy, especially for high-precision work where subtle shifts become critical [1-4].

The geometric tolerances in manufacturing require trazable dimensional metrology to guarantee the production quality [5,6]. The behaviour of the manufacturing systems can be improved through verification and compensation techniques [2]. There are different ways to perform a machine tool (MT) verification: measuring the movement of each axis with an interferometer [7]; measuring circular paths with a ball-bar [8]; measuring the displacement of the head with a laser tracker [9] or triangulating distances that are measured from several points on the MT bed plate to a point fixed to the MT head using laser tracers [10] and laser ball-bars [11, 12], this last method usually requires several cycles modifying the position of the equipment fixed on the bed plate of the MT.

In any of these processes, temperature changes that occur during the use of measuring instruments affect the accuracy and repeatability of the measurement result. Temperature variations occur both during equipment setup and data acquisition during verification, impacting the results of the verification and compensation of the production system.

This paper studies the influence of temperature on the measurement results of an instrument based on interferometry and simultaneous multilateration. The instrument, classified within the group of laser ball-bars, consists of a telescopic simultaneous ball bar (TSB), composed of three telescopic arms, which simultaneously measures the distances between three fixed spheres and a single sphere located on the headstock of a machine tool or robot—the manufacturing system under inspection. This work models the measurement process and the influence of temperature from the initial steps, which allow for the adjustment of each telescopic ball-bar (TB), to obtaining the measurement results, also modeling the intermediate steps, such as measuring the distance between the three fixed spheres with the TSB.

The TSB has been analyzed in previous works: [13] presents an evaluation of the uncertainty with TSB calibration and [14] shows the use of the system and a comparison of its measurement results with an interferometer. This work complements these studies, focusing on evaluating the influence of temperature on the measurement uncertainty of the TSB.

The paper is structured as follows: Section 2 describes the TSB, its measurement procedure, and the errors associated with the effect of temperature. Section 3 details the methodology followed in the analysis and the configuration of each simulated test. Section 4 presents the results obtained from the study that isolate the effect of temperature on TSB measurement results. Finally, Section 5 presents the main conclusions of the study.

## 2. Hardware model and measurement procedure

This section describes the use of a TSB to measure 3D coordinates of a point in space multilaterating from the distances between the point under measurement and three fixed points located on the bed plate of the system. The main effects due to temperature changes during the set up and the measurement process are also described.

### *2.1. Telescopic simultaneous ball-bar*

The TSB measure 3D coordinates of a point in space. The TSB is composed by three TB. Each TB measures the distance between two steel spheres using an interferometer. The special design of each TB allows three ends pointing to the same steel sphere while the other end of each TB is located in a fixed kinematic support, KS [15]. This configuration allows the simultaneous tracking of a steel spheres with the TSB: three TB simultaneously measuring the distance between three fixed points (the kinematic supports, $KS_i$, with $i$ from 1 to 3) and the steel sphere, figure 1.

From the three distances between spheres measured simultaneously, $L_{i,p}$ with $i$ from 1 to 3, by each TB of the TSB, the coordinates of the centre of the steel sphere, $P$ ($P$ = $\{X\ Y\ Z\}'$), can be multilatered as shown in (1) to (3).

$$X = \frac{{L_{1,p}}^2 - {L_{2,p}}^2 + {X_{KS2}}^2}{2 \cdot X_{KS2}} \tag{1}$$

$$Y = \frac{{L_{1,p}}^2 - {L_{3,p}}^2 + {X_{KS3}}^2 + {Y_{KS3}}^2}{2 \cdot Y_{KS2}} - \frac{X_{KS3}}{Y_{KS3}} \cdot X \tag{2}$$

$$Z = \sqrt{{L_{1,p}}^2 - X^2 - Y^2} \tag{3}$$

Where. $X_{KSi}$ $Y_{KSi}$ $Z_{KSi}$, with $i$ from 1 to 3, are the coordinates of the centre of the sphere located in each kinematic support (KS) expressed in the TSB reference system ($RS_{TSB}$), (4) to (6).

$$X_{KS} \ = L_{12} \tag{4}$$

$$X_{KS3} = L_{13} \cdot \cos(\beta_{13}) \tag{5}$$

$$Y_{KS3} = L_{13} \cdot \sin(\beta_{13}) \tag{6}$$

Where $\beta_{13}$ is the angle between the segment joining KS1 and KS3 with the segment joining KS1 and KS2 (Figure 1) and its cosine can be calculated from the cosine theorem with the three distances between the KSs ($L_{i,j}$,with i≠j and i,j form 1 to 3), (7). The remaining values that do not appear in (4) to (6) are zero.

$$\cos(\beta_{13}) = \frac{L_{2,3}^2 - L_{1,2}^2 - L_{1,3}^2}{-2 \cdot L_{1,2} \cdot L_{1,3}} \tag{7}$$

### *2.2. Measurement procedure*

The first step of the procedure (STEP1) is to set up the reference distance for the interferometer of each TB. A calibrating ball beam artifact (CBBA) is used to materialice the reference distance, $L_0$, with an uncertainty of 1.3 µm with a coverage factor k=2 in accordance with the Guide to the Expression of Uncertainty in Measurement, GUM [16].

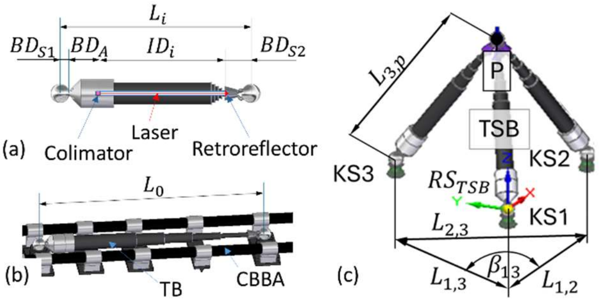


**Figure 1.** (a) TB: Balance distance, $BD_S = BD_{S1} + BD_{S2}$, and interferometer distance, $ID_i$. Both distances make up the resulting distance between spheres. (b) Set up of a TB with the CBBA in the reference position, $L_0$. (c) TSB mode. Reference systems and characteristics of the TSB: $RS_{TSB}$, KC, $L_{i,j}$ (measured in the second step of the measurement procedure) and $L_{i,p}$ (measured in the third step).

The interferometer measures the distance between spheres with an offset (balance distance, BD) due to its integration into the TB (Interferometer distance, ID), (8).

Once each TB is set up with $L_0$, the distance obtained from the laser interferometer is the increment from $L_0$, (9), and the distance between spheres need to be internaly computed. This aply for the following steps (second and third).

$$L_0 = BD + ID_0 \tag{8}$$

$$L_i = BD + ID_0 + \Delta ID_i \tag{9}$$

$$BD = BD_S + BD_A = BD_{S1} + BD_{S2} + BD_A \tag{10}$$

Where $BD_S$ and $BD_A$ are the lengths of the balance distance manufactured with steel (54%) and aluminium alloy (46%) respectively.

The second step (STEP2) is the measurement of the distances between the fixed KS, $L_{i,j}$. Each TB measures simulateously one of the three $L_{i,j}$.

The third step (STEP3) is the measurement of $L_{i,p}$. In this step each TB measures simulateously the distance between a KS and the sphere in the manufacturing system head, P.

At each measurement step environmental temperature, ET, and the temperatures of the machine and the TSB are recorded along with each measurement.

Finally, STEP4, is the reconstruction of the 3D coordinates of P from (1) to (7).

### *2.3. Effect of the temperature in the measurement procedure*

In a temperature-controlled environment where working temperature can be assumed to coincide with reference temperature ($T_R = 20°C$), (9) can be rewritten as equation (11).

$$L_i = L_0 + \Delta ID_i \tag{11}$$

However, temperatures other than $T_R$ modify the dimensions of the materials according to their coefficient of thermal expansion. For the materials analyzed, their coefficient of linear thermal expansion (CLTE) was considered with a constant value within the operating temperature range (Table 1).

**Table 1.** Coeficients of linear thermal expansion (CLTE) and estimated uncertainty according to ISO 230 [17].

| Material | CLTE $/K^{-1}$ | $\sigma = u_{CLTE}\ /K^{-1}$ |
|---|---|---|
| **Aluminium Alloy ($\alpha_A$)** | $23.00 \cdot 10^{-6}$ | $0.66 \cdot 10^{-6}$ |
| **Steel ($\alpha_S$)** | $11.00 \cdot 10^{-6}$ | $0.58 \cdot 10^{-6}$ |
| **Carbon Fiber ($\alpha_{CF}$)** | $-0.74 \cdot 10^{-6}$ | $0.58 \cdot 10^{-6}$ |
| **Machine Tool ($\alpha_M$)** | $12.00 \cdot 10^{-6}$ | $0.58 \cdot 10^{-6}$ |

In STEP1 the CBBA dimension depends on the artifact temperature ($T_a$) and the material used for its manufacturing, in this case carbon fiber. The interferometer reading in STEP1 ($ID_0$) will depend on the CBBA dimension and the BD dimension at the TB temperature during setup ($T_{TB}$). Since the adjustment must be performed on-site prior to taking measurements, $ID_0$ will be affected by the temperature, (12).

$$L_0(1 + \alpha_{CF}\theta_a) = BD_S(1 + \alpha_S\theta_{TB}) + BD_A(1 + \alpha_A\theta_{TB}) + ID_0(1 + \alpha_{CF}\theta_a) \tag{12}$$

$$\theta_i = T_i - T_R \tag{13}$$

$$ID_0 = L_0 - \frac{BD_S(1 + \alpha_S\theta_{TB}) + BD_A(1 + \alpha_A\theta_{TB})}{(1 + \alpha_{CF}\theta_a)} \tag{14}$$

$$\begin{aligned} L_i(1 + \alpha_M\theta_{Mi}) = \quad & BD_S(1 + \alpha_S\theta_{TBi}) \\ & + BD_A(1 + \alpha_A\theta_{TBi}) \\ & + ID_0(1 + \alpha_{CF}\theta_a) \\ & + \Delta ID_i(1 + \alpha_M\theta_{Mi}) \end{aligned} \tag{15}$$

During setup, STEP1, the CBBA and TSB temperatures are $T_a$ and $T_{TB}$ respectively.

In the next steps, after STEP1, the measurement provided by the interferometer as a function of temperature, $T_{Mi}$, ($\Delta ID_i(1 + \alpha_M\theta_{Mi})$; where $\alpha_M$ is the CLTE of the machine tool and $\theta_{Mi}$ is the diference between, $T_{Mi}$, the temperature of the machine tool and $T_R$) is used to calculate the value of the length measured between spheres, $L_i$, (15),

After STEP2 and STEP3, $L_{i,j}$ and $L_{i,P}$ are calculated, (15), and used to obtain the 3D coordinates of P with (1) to (7).

## 3. Methodology and simulation test

The thermal effect in the uncertainty of a length measurement can be modelled, according with ISO/TR 16015 [18], from three main uncertainty components: the effect of the ET variation, the effect of the uncertainty of each CLTE and the effect of the uncertainty in the measurement of the temperature.

The variation of the ET during the measurement process, which lasts approximately 40 minutes, is defined, based on previous experiments, as 1°C from the beginning to the end of the measurement process. To simulate this effect, a temperature curve is defined that follows (16) with k = 0.05 $min^{-1}$.

$$T_i = T_{out} + (T_{ini} - T_{out})e^{-kt} \quad (16)$$

The outside temperature of the workshop, $T_{out}$, is randomly selected between 14 and 27 °C in each iteration. The initial temperature, $T_{ini}$, is randomly selected with an increment of $\pm 0.5\ °C$ relative to $T_{out}$ in each iteration. (16) estimates the ET for each step described: In STEP 1, an ET is established for the adjustment of each TB ($T_{0,1} = T_i(t=1)$, $T_{0,2} = T_i(t=2)$, $T_{0,3} = T_i(t=3)$, with t in minutes). In STEP 2, $T_{i,j} = T_i(t=4)$, because the three distances are measured simultaneously, $L_{i,j}$,with i≠j and i,j form 1 to 3. In STEP 3, an ET is estimated for each of the 214 points of the VV ($T_{i,P}$,= $T_i(t)$, with t increasing by 10s for each measured point).

Following the measurement procedure in section 2.2, the model establishes a temperature for each element of the system involved in the process, based on the estimated ET for each step. Temperature influences the dimensions of the materials according to their CLTE and the uncertainty of the CLTE estimate influences the uncertainty of the length measurement. Table 1 shows the CLTE and its estimated uncertainty according to ISO 230 [17]. In the simulation, the CLTE uncertainty is modelled by introducing normally distributed noise to the CLTE value identified for each material.

Environmental compensation unit (ECU) calibration allows for the correction of systematic error in temperature measurement, but the measurement uncertainty, although known, will introduce an error into the compensation model. To simulate the temperature measurement uncertainty the model generates normally distributed noise ($\sigma = U_{ECU}/k_{ECU}$) for each temperature measured in the process. From the ECU calibration $U_{ECU} = 0.01\ °C$ and a coverage factor $k_{ECU} = 2$ are obtained, in accordance with the GUM [16].

The simulation model calculates $\Delta ID_i$ using nominal values for the temperature (17). $\Delta ID_i$ is used to recalculate the $L_i'$ values. $L_i'$ values correspond to the $L_i$ values calculated introducing noise into the temperature data to simulate the uncertainty in the measurement of the temperature (18).

$$\Delta ID_i = L_i - \frac{BD_S(1+\alpha_S\theta_{TBi}) + BD_A(1+\alpha_A\theta_{TBi}) + ID_0(1+\alpha_{CF}\theta_a)}{(1+\alpha_M\theta_{Mi})} \quad (17)$$

$$L_i' = \Delta ID_i + \frac{BD_S(1+\alpha_S\theta_{TBi}') + BD_A(1+\alpha_A\theta_{TBi}') - ID_0(1+\alpha_{CF}\theta_0')}{(1+\alpha_S\theta_{Mi}')} \quad (18)$$

From (17) and (18) the simulated values $L_{i,j}'$ and $L_{i,P}'$ are obtained allowing the 3D reconstruction of the coordinates of $P'$. The coordinates of $P'$ are compared with the nominal value of $P$ obtaining an error value for each point, (19) and (20).

$$XYZ_{Error}' = XYZ' - XYZ \quad (19)$$

$$D_{Error}' = \sqrt{(X' - X)^2 + (Y' - Y)^2 + (Z' - Z)^2} \quad (20)$$

With the aim of understanding the thermal effect in the case where the thermal expansion of the materials is not compensated for, a second model is proposed (21) to (23).

$$L_i'' = \Delta ID_i + L_0 \quad (21)$$

$$XYZ_{Error}'' = XYZ'' - XYZ \quad (22)$$

$$D_{Error}'' = \sqrt{(X'' - X)^2 + (Y'' - Y)^2 + (Z'' - Z)^2} \quad (23)$$

The verification volume (VV) consists of 214 points, distributed with varying TB lengths from 500 mm in 100 mm increments to a maximum of 1000 mm so that a representative VV of the TSB is covered.

The effect of the temperature in the measurement uncertainty of the TSB is estimated using the Monte Carlo Method [19].

The number of iterations is an important parameter of the Monte Carlo simulation. From previous works, the Monte Carlo simulation converge using $10^6$ iterations [13].

The simulation model allows the thermal influence on the measurement uncertainty estimate for the TSB to be isolated. The results are compared with the nominal values and with those obtained without temperature compensation.

## 4. Simulation results

Following the methodology exposed in the previous section the simulation has been performed. The $10^6$ iterations to apply the Monte Carlo Method took 540 s with a 3.0 GHz CPU clock speed.

The effect of length measurement errors on reconstructing the coordinates of measured points depends on the location of the points within the VV. Since the effect of temperature on the measurement result is to introduce errors in the measurement of lengths, the magnitude of its influence varies depending on the area of the VV in which the measured point is located.

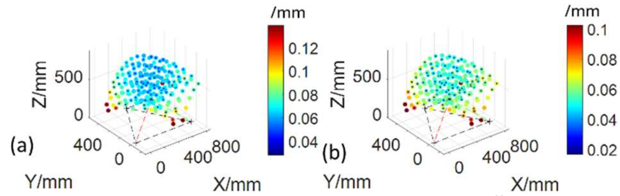


**Figure 3.** (a) Error distribution (maximum value of $D_{Error}''$ for each point) in the TSB VV. (b) Distribution in the VV of the uncertainty (maximum value of the triple: Uncertainty of X, Y and Z) due to the lack of temperature compensation in the measurement process.

Figure 3 shows the error distribution in the TSB VV and the effect on uncertainty as the calculated uncertainty value when only the effect of temperature is considered. For the proposed variations, between 14 and 27 °C, the error introduced in the reconstruction of the point coordinates reaches 139 µm ($XYZ_{Error}''$ and $D_{Error}''$), while the effect on the estimated uncertainty in the coordinate reconstruction reaches 102 µm.

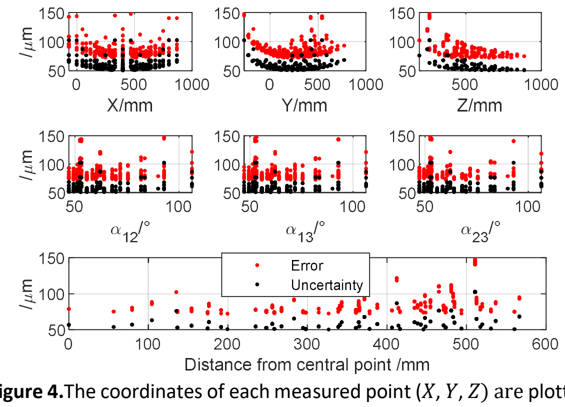


**Figure 4.**The coordinates of each measured point ($X, Y, Z$) are plotted in the abscissa in the first row, the angles formed by the TBs in the second row, and the distance from the central point in the third row versus the maximum value of $D_{Error}''$ for each point (red) and the estimated uncertainty (maximum value of the triple: Uncertainty of X, Y and Z) for each point in ordinates (black).

The error and uncertainty trend as a function of the coordinates, as a function of the angles formed by the TBs and as a function of the distance to the central point of the TSB (point where the arms form a trirectangular trihedron, represented by an asterisk in Figure 2 b) is represented in Figure 4.

When temperature is compensated, the error decreases so that the effect on the measurement results is limited. By compensating for temperature, the error in the reconstruction of the points ($XYZ'_{Error}$ and $D'_{Error}$) is reduced to 11 µm. The effect on the measurement uncertainty is below 7 µm (Figure 5).

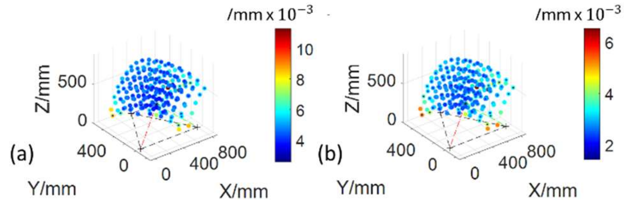


**Figure 5.** (a) Error distribution (maximum value of $D'_{Error}$ for each point) in the TSB VV. (b) Distribution in the VV of the uncertainty (maximum value of the triple: Uncertainty of X, Y and Z) due to the uncertainty in the measurement of temperature for its compensation in the measurement process.

The error and uncertainty trend for the case where the temperature effect is compensated can be seen in Figure 6.

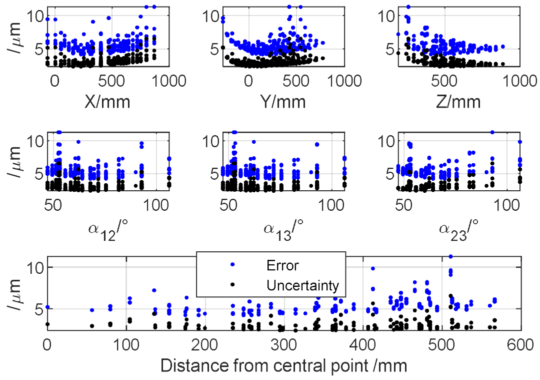


**Figure 6.** The coordinates of each measured point $(X, Y, Z)$ are plotted in the abscissa in the first row, the angles formed by the TBs in the second row, and the distance from the central point in the third row versus the maximum value of $D'_{Error}$ for each point (blue) and the estimated uncertainty (maximum value of the triple: Uncertainty of X, Y and Z) for each point in ordinates (black).

Table 2 shows the effect of temperature compensation on the uncertainty and the measurement error.

**Table 2.** Main effects on uncertainty and thermal errors obtained from the simulation. Temperature compensation is obtained from equations (17) to (20), $XYZ'_{\square}$. Values without temperature compensation are obtained from equations (21) to (23), $XYZ''_{\square}$.

| /µm | Uncertainty | | | Thermal erorrs | | |
|---|---|---|---|---|---|---|
| | X | Y | Z | X | Y | Z |
| $XYZ''_{\square}$ | 36.3 | 24.4 | 102.5 | 52.8 | 41.2 | 138.9 |
| $XYZ'_{\square}$ | 2.8 | 2.5 | 6.5 | 5.0 | 4.8 | 11.3 |

## 4. Conclusions

When the temperature deviates from the reference value, systematic errors are introduced into the measurement process if their effects are not compensated. Furthermore, uncertainty in temperature measurement propagates into length measurements, increasing overall measurement uncertainty and degrading the accuracy of point coordinate reconstruction.

The proposed model effectively compensates for temperature-induced effects, reducing both measurement uncertainty to 6.5 µm and systematic measurement error to 11.3 µm.

Future work will focus on characterizing temperature effects when additional materials commonly used in production systems are involved, such as aluminum-based structures.

**Acknowledgments:** This research was funded by the Ministerio de Ciencia e Innovación with project number PID2022-139280OB-I00, by Aragon Government (Department of Industry and Innovation) through the Research Activity Grant for research groups recognized by the Aragon Government (T56_17R Manufacturing Engineering and Advanced Metrology Group). This is co-funded with European Union ERDF funds.

**References**

[1] Swyt DA. Uncertainties in Dimensional Measurements Made at Nonstandard Temperatures. J Res Natl Inst Stand Technol. 1994 Jan-Feb; **99**(1):31-39. doi: 10.6028/jres.099.004.

[2] Schwenke H, Knapp W, Haitjema H, Weckenmann A, Schmitt R, Delbressine F 2008 Geometric error measurement and compensation of machines – An update *CIRP Ann.* **57** (2) 660-75, https://doi.org/10.1016/j.cirp.2008.09.008.

[3] Ferrucci M, Haitjema H, Leach R 2018 Chapter: Dimensional Metrology in: Basics of Precision Engineering (R. Leach, S. T. Smith, R. Leach, S.T. Smith, Boca Raton), CRC Press, 151-203 978-1-4987-6085-0.

[4] De Groot P, Badami V, Liesener J 2016 Concepts and geometries for the next generation of heterodyne optical encoders *Proc. ASPE* (Portland, Oregon) **65** 146–149.

[5] Moona G,Jewariya M, Sharma R 2019 Relevance of Dimensional Metrology in Manufacturing Industries *MAPAN* **34** (1) 97–104, https://doi.org/10.1007/s12647-018-0291-3.

[6] BIPM, IEC, IFCC, ILAC, ISO, IUPAC, IUPAP, OIML 2008 International vocabulary of metrology—Basic and general concepts and associated terms, JCGM 200 Bureau International des Poids et Mesures (BIPM), 2008.

[7] Jiang X, Meng T, Wang L, Liu C 2020 Rapid calibration method for measuring linear axis optical paths of computer numerical control machine tools with a laser interferometer *Int. J. Adv. Manuf. Technol.* **110** 3347-64, https://doi.org/10.1007/s00170-020-05976-6.

[8] Zhong L, Bi Q, Wang Y 2017 Volumetric accuracy evaluation for five-axis machine tools by modeling spherical deviation based on double ball-bar kinematic test *Int. J. Mach. Tools Manuf.* **122** 106-19, https://doi.org/10.1016/j.ijmachtools.2017.06.005.

[9] Aguado S, Samper D, Santolaria J, Aguilar J J 2012 Identification strategy of error parameter in volumetric error compensation of machine tool based on laser tracker measurements *Int. J. Mach. Tools Manuf.* **53** (1) 160-9, https://doi.org/10.1016/j.ijmachtools.2011.11.004.

[10] Zha J,Wang T,Li L, Chen Y 2020 Volumetric error compensation of machine tool using laser tracer and machining verification *Int. J. Adv. Manuf. Technol.* **108** (7- 8) 2467-81 https://doi.org/10.1007/s00170-020-05556-8.

[11] Fan K C, Wang H, Shiou F J, Ke C W 2004 Design analysis and applications of a 3D laser ball bar for accuracy calibration of multiaxis machines *J. Manuf. Syst.* **23** (3) 194-203 https://doi.org/10.1016/S0278-6125(05)00009-9.

[12] Etalon X-AX LASERBAR, https://www.etalonproducts.com/en/products/x-ax_laserbar/, 2021 (Accessed: January 2024).

[13] Brosed F J, Aguilar J J, Acero R, Santolaria J, Aguado S, Pueo M 2022 Calibration and uncertainty budget analysis of a high precision telescopic instrument for simultaneous laser multilateration *Measurement* **190** 110735. https://doi.org/10.1016/j.measurement.2022.110735.

[14] Acero R, Brosed F J, Pueo M, Aguado S, Aguilar J J, Velazquez J, Evaluation of a telescopic simultaneous ballbar in a 3-axis machine tool using a reference equipment, Precision Engineering, **88**, 2024, 117-124, ISSN 0141-6359, https://doi.org/10.1016/j.precisioneng.2024.02.001.

[15] Acero R, Aguilar J J, Brosed F J, Santolaria J, Aguado S, Pueo M 2021 Design of a Multi-Point Kinematic Coupling for a High Precision Telescopic Simultaneous Measurement System *Sensors* **21** 6365 https://doi.org/10.3390/s21196365.

[16] BIPM, IEC, IFCC, ILAC, ISO, IUPAC, IUPAP, OIML 2008 Evaluation of Measurement Data—Guide to the Expression of Uncertainty in Measurement, JCGM 100 Bureau International des Poids et Mesures (BIPM), 2008.

[17] International Organization for Standardization (ISO) 2012 Machine Tools. Test code for machine tools—ISO 230. ISO.

[18] International Organization for Standardization. (2003). Geometrical product specifications (GPS)—Systematic errors and contributions to measurement uncertainty (ISO/TR 16015:2003). ISO.

[19] BIPM; IEC; IFCC; ILAC; ISO; IUPAC; IUPAP; OIML 2008 Evaluation of Measurement Data—Supplement 1 to the Guide to the Expression of Uncertainty in Measurement—Propagation of Distributions Using a Monte Carlo Method; JCGM 101 Bureau International des Poids et Mesures (BIPM), 2008.